Fizika Nizkikh Temperatur, 2002, v. 28, No. 11, p. 1138–1149

Fluctuation conductivity in Y–Ba–Cu–O films with artificially produced defects

A. L. Solovjov

B. Verkin Institute for Low Temperature Physics and Engineering, National Academy of Sciences of Ukraine, 47 Lenin Ave., 61103 Kharkov, Ukraine
E-mail: solovjov@ilt.kharkov.ua

Received March 14, 2002

The fluctuation-induced conductivity (paraconductivity) measured in $YBa_2Cu_3O_{7-\delta}$ (YBCO) films grown on 10° miscut $SrTiO_3$ (001) substrates is analyzed using various theoretical models describing weak fluctuations in high-T_c superconductors and considering both Aslamazov–Larkin and Maki–Thompson fluctuation contributions in the clean limit approach. The analysis reveals a highly anisotropic pair-breaking caused by structural defects produced. This result is in favor of an idea that pseudogap in high-T_c oxydes is mainly governed by the fluctuating pairing.

PACS: **74.40.+k**

1. Introduction

The pseudogap (PG) phenomenon in high-T_c superconductors (HTSC) is widely debated at present [1]. Measurements taken with a wide variety of techniques demonstrate that the pseudogap is present in both the spin and charge channel but theoretical views of the problem are still rather controversial. One point of view which stands out in the context of experimental evidence is the idea of preformed pairs [1] considered to be the fluctuating Cooper pairs which are believed to be present in HTSC well above T_c [2,3]. As structural defects are known to deeply affect the pair-breaking mechanism in high-T_c oxides [2], investigation of the influence of systematically produced structural defects on the fluctuation conductivity is to clarify the issue.

Measurement of the fluctuation conductivity (FC) is known to be a powerful method of getting reliable information about the normal charge scattering and superconducting coupling mechanisms in HTSC just in the PG temperature region [4–11]. Using FC analysis, such microscopic parameters as the coherence length along the c axis, $\xi_c(0)$, and the phase relaxation time of fluctuating pairs, $\tau_\varphi(100\ \mathrm{K})$, can be determined. It also gives the possibility to address more fundamental issues such as the contribution from or absence of Maki–Thompson (MT) type fluctuations [12]. The question is of remarkable importance, since the MT fluctuation process is strongly dependent on the pairing mechanism [12,13].

Fluctuation conductivity, $\sigma' = \sigma(T) - \sigma_N(T)$, arises from excess current carried by fluctuation-created Cooper pairs above the superconducting transition temperature T_c, as has been shown by Aslamazov and Larkin (AL) [14]. The additional contribution to FC, introduced by Maki and Thompson [12] to extend the AL theory, is treated as arising from interaction of the fluctuating Cooper pairs with normal electrons resulting in the pair-breaking process. Finally, the fluctuation conductivity is taken to be

$$\sigma'(T) = [\rho_N(T) - \rho(T)]/[\rho_N(T)\rho(T)]\,, \qquad (1)$$

where $\rho(T) = \rho_{xx}(T)$ is the actually measured longitudinal resistivity and $\rho_N(T) = \alpha T + b$ is the extrapolated normal-state resistivity. According to the nearly antiferromagnetic Fermi liquid (NAFL) model [15] the linear-in-T $\rho_{xx}(T)$ dependence at high temperatures can be considered as a true sign of the normal state of the system, a state which is characterized by stability of the Fermi surface and, hence, by stability of the normal-carrier scattering rate. As T is lowered, $\rho_{xx}(T)$ deviates downward from the T-linear dependence at some representative temperature $T_{*0} >> T_c$, giving rise to the excess conductivity which is usually considered as a

pseudogap [1,15]. However, in the temperature interval $T_c < T < T_{c0}$ the excess conductivity is well described by the conventional fluctuating theories [12–14] and is usually treated as $\sigma'(T)$ [4–10,16]. $T_{c0} = (100 \pm 5)$ K is the temperature which determines the pair-breaking parameter $\delta_{th} = (T_{c0} - T_c)/T_c$ [12,13]. The possibility of the fluctuating pairing in HTSC at $T_{c0} < T < T_{*0}$ is widely debated at present [1–3].

As we have recently shown [16], the $\sigma'(T)$ dependence of well-structured optimally doped (OD) and strongly underdoped (UD) YBCO films always consists of two temperature regions with different FC behavior, separated by the dimensional crossover at T_0. Accordingly, above T_0 this is the two-dimentional (2D) fluctuation region commonly described by the MT term of the Hikami–Larkin theory (HL) [13], and at $T_c < T < T_0$ it is the region of three-dimentional (3D) fluctuations always described by the 3D term of the AL theory [14]. The Lawrence–Doniach (LD) model [17], proposed to describe FC in any layered superconducting system, was found to fail in fitting experiment in this case. Really, the LD model predicts a smooth, gradual transition from 2D AL fluctuation behavior to 3D AL behavior as the temperature approaches T_c, and it considers the MT contribution to be vanishing. This kind of FC behavior has been shown to be typical for badly structured high-T_c oxides [2]. However, in most of the previous papers devoted to the problem, FC fitted by the LD model alone is reported [4–9], suggesting the presence of different structural defects in the samples studied. The conclusion is corroborated by measurements of the critical current densities j_c of thin epitaxial YBCO films, which are known to be at least an order of magnitude larger than that for high-quality YBCO single crystals [18]. The main reason for that is strong flux pinning in the films caused by specific defects such as point defects in the CuO_2 planes [19], screw dislocations [20], and twin boundaries [21], expected to be also responsible for observed $\sigma'(T)$ dependence of the LD type. However, the properties of high-quality modern thin epitaxial HTSC films prepared by pulsed laser deposition [22] are believed to be mostly determined by some slight degree of miscut growth of the films, resulting in the appearance of specific growth-related defects [23,24]. These defects have been identified as effective pinning centers [23] and have been found to produce an appreciable anisotropy of the resistivity, magnetic flux penetration, and critical current densities in miscut-grown YBCO films [24]. However, a systematic study of the effect of specific growth-related defects on the fluctuating pairing in HTSC is still lacking.

In this paper we presented measurements of the fluctuation conductivity in the *c*-axis-oriented $YBa_2Cu_3O_{7-\delta}$ (YBCO 123) films grown on 10° miscut $SrTiO_3$ (001) substrates. The expected strong anisotropy of the scattering of the fluctuating pairs due to growth-related defects influence is revealed. The results are treated using a recently developed approach to FC analysis in YBCO films [2,16].

2. Experimental techniques

YBCO films with a thickness of 240 to 2400 Å were grown on vicinal $SrTiO_3$ (001) substrates by pulsed laser deposition (PLD) as described in detail in Ref. 24. The $SrTiO_3$ substrates were cut and polished 10° off the (001) plane towards [010], as confirmed by Laue diffraction. After the PLD process the deposition chamber was pumped to a pressure of less than 10^{-7} mbar and the samples were transferred to the scanning tunneling microscopy (STM) stage without exposure to air. To provide measurements of expected resistivity anisotropy the samples were patterned in two different directions. These two directions are denoted in the text by **L** and **T**, respectively, since they coincide with the directions longitudinal to and transverse to the film step edges. To get the resistivity data, standard 4-probe dc measurements were performed using a fully computerized setup. It should be emphasized that a certain care in the sample preparation process enables to obtain highly reliable and systematic data despite the evident complexity of the samples' structure.

Combined STM and cross-sectional transmission electron microscopy (TEM) measurements established a close relationship between the film morphology and defect microstructure [24]. It has been shown that almost periodic surface and defect structure is generated for YBCO films grown on 10° miscut $SrTiO_3$ substrates. The TEM image has revealed a significantly disturbed YBCO lattice. The step structure persists on the YBCO surface due to the step flow growth mechanism. This generates a multitude of translational boundaries (TB), extending throughout the entire film thickness. The crystal lattice is slightly tilted across the defects. Numerous stacking faults (SF) are also created, resulting in a general waviness of the unit-cell-high layers as observed in the TEM image. A strong strain field is associated with this specific defect structure. Some extended defects (ED) with a structural width of 20–30 Å, penetrating most of

the film thickness, are also present. All defects, and especially TB, are found to contribute to the strong flux pinning in the films. It has also been shown [24] that the close correspondence between the STM and TEM results suggests that most defects are aligned along the direction **L** of the regular film step edges. This one-dimentional nature of the defects is found to be resposible for observed anisotropy of the resistivity, magnetic flux penetration, and critical current densities [24]. Naturally, one can expect to reveal an anisotropy of the pair-breaking mechanism in the films, resulting in the anisotropy of the fluctuation conductivity. If pseudogap in high-T_c oxides is really governed by the fluctuating pairing different temperature regions of the PG behavior have to be observed, depending on whether measurements are perfomed in the **L** or in **T** direction.

3. Results and discussion

3.1. Transport properties

To obtain more information, two films with different thicknesses commonly used in experiment, d_0 = 1900 Å (sample M23) and d_0 = 900 Å (sample M35), were chosen for analysis. Both films exhibit a sharp resistive transition at $T_c \approx 90$ K in both directions (see the Table), i.e., can be considered as apparent representatives of OD YBCO systems. Figure 1 shows ρ_{xx} as a function of temperature for sample M23 measured in the **L** and **T** directions, respectively. As can be readily seen, $\rho_{\mathbf{T}}(100\,\mathrm{K})/\rho_{\mathbf{L}}(100\,\mathrm{K}) \approx 3.2$ in this case. Moreover, a value $\rho_{\mathbf{T}}(100\,\mathrm{K})/\rho_{\mathbf{L}}(100\,\mathrm{K}) \approx 9.5$ is measured for sample M35, suggesting the strong influence of the growth-related defects on the normal charges scattering. However, despite of the considerable increase of the resistivity, the width of the resistive transition $\Delta T \approx 1.2$ K is estimated for M23 in both directions (Table), a value typical for well-characterized OD systems. The representative temperature $T_{*0\mathbf{L}}$, marked by the arrow on the graphs, is also found to be in good agreement with the prediction of the NAFL model for OD films. According to the NAFL model, the **T**-linear resistivity above T_{*0}, extrapolated towards T_c (as shown by the dashed lines in the figure), is treated as the sample normal-state resistivity $\rho_N(T)$ used to determine $\sigma'(T)$ from Eq. (1). However, resistivity buckling, which is uncharacteristic of OD systems, is distinctly observed for both samples at higher temperatures (Fig. 1). The result suggests the presence of a somewhat enhanced electron–electron interaction in the films [15], likely caused by the defect structure.

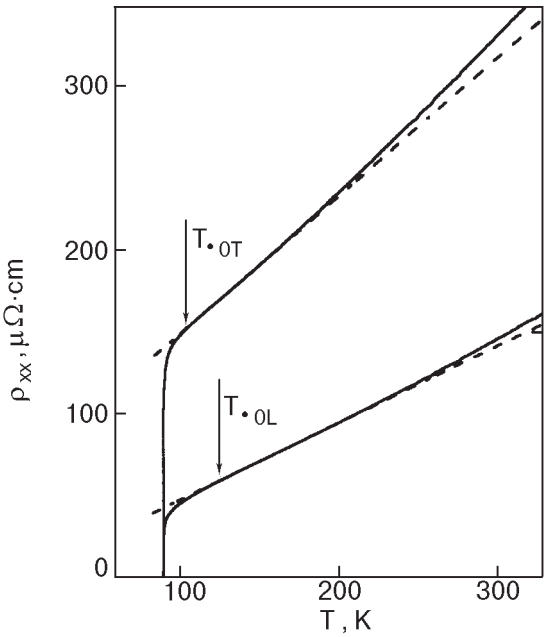

Fig. 1. Resistivity as a function of temperature for sample M23 measured in the **L** and **T** direction; the dashed lines is the extrapolated normal-state resistivity.

But the most striking result is the fact that measured for both films representative temperatures $T_{*0\mathbf{L}}$ and $T_{*0\mathbf{T}}$ appear to be noticeably different (Fig. 1 and the Table). As it is clearly seen from the figure, the larger resistivity, the shorter is the **T**-linear resistivity region but the shorter becomes the PG temperature range too, what is difficult to explain in terms of the normal charges scattering only. To account for the finding, measurements of

Table

The sample parameters

Sample	d_0, Å	T_c, K	ΔT, K	T_c^{mf}, K	ρ(100K), μΩ·cm	ρ(300K), μΩ·cm	$d\rho/dT$, μΩ·cm·K^{-1}	T_{*0}, K
M23-**L**	1975	90.0	1.0	90.14	88	287	0.93	130
M23-**T**	1900	89.9	1.2	90.19	278	628	1.6	108
M35-**L**	900	89.7	2.0	90.60	204	600	1.86	150
M35-**T**	900	89.5	2.2	90.85	1948	3325	6.06	105

FC, sheding light on the fluctuating pairing, are evidently required.

3.2. Fluctuation conductivity

3.2.1. Theoretical overview. The fluctuation conductivity $\sigma'(T)$ is computed from the resistivity measurements (Fig. 1) using Eq. (1), as discussed above. The experimental FC data are analyzed using the HL theory [13], considering both the AL and MT fluctuation contributions. In the absence of magnetic field **H** the AL theory yields

$$\sigma'_{AL} = [e^2/(16\hbar d)](1+2\alpha)^{-1/2}\varepsilon^{-1} \qquad (2)$$

and

$$\sigma'_{MT} = \frac{e^2}{8\hbar d(1-\alpha/\delta)} \times \times \ln\left\{\frac{(\delta/\alpha)[1+\alpha+(1+2\alpha)^{1/2}]}{[1+\delta+(1+2\delta)^{1/2}]}\right\}\varepsilon^{-1}, \qquad (3)$$

where $d \approx 11.7$ Å is the distance between conducting CuO_2 planes, $\alpha = 2\xi_c^2(T)/d^2 = 2[\xi_c(0)/d]^2\,\varepsilon^{-1}$ is a coupling parameter,

$$\delta = 1.203(l/\xi_{ab}(0))(16/\pi\hbar)[\xi_c(0)/d]^2 k_B T\tau_\varphi \quad (4)$$

is a pair-breaking parameter, and $\varepsilon = \ln(T/T_c^{mf}) \approx \approx (T-T_c^{mf})/T_c^{mf}$ is a reduced temperature. Here $T_c^{mf} > T_c$ is the critical temperature in the mean-field approximation actually separating the FC region from the critical fluctuation region. The factor $1.203(l/\xi_{ab}(0))$ (Eq. (4)) is introduced by Bieri, Maki, and Thompson (BMT) [25], who have extended the HL theory to incorporate the clean limit approximation. This seems to be reasonable, as the mean free path $l > \xi_{ab}(0)$ for YBCO systems, where $\xi_{ab} > \xi_c$ is the intraplane coherence length. But when $\mathbf{H} = 0$ the only difference with the HL theory is that $\delta_{BMT} = 1.203(l/\xi_{ab}(0))\delta_{HL}$, assuming that nonlocal effects can be ignored [25].

Actually, Eq. (2) reproduces the result of the LD model [17], with allowance for the presence of Josephson-like pair tunneling between conducting layers [26], which is mainly pertinent to the 3D region, as $\xi_c(T) > d$ near T_c. Accordingly, the MT contribution gains importance at $k(T-T_c^{mf}) >> \hbar/\tau_\varphi$ [13], where no intraplane tunneling is expected, as $\xi_c(T) < d$ (2D region) [10,26]. Thus the HL theory predicts both 2D–3D and MT–LD crossovers as the temperature approaches T_c. The 2D–3D crossover should occur at the temperature

$$T_0 = T_c\{1+2[\xi_c(0)/d]^2\} \qquad (5)$$

at which $\alpha = 1/2$, i.e., $\xi_c(0) = (d/2)\,\varepsilon_0^{1/2}$. The MT–LD crossover should occur at the temperature

$$\varepsilon_0 = (\pi\hbar)/[1.203(l/\xi_{ab}(0))(8k_B T\tau_\varphi)], \qquad (6)$$

where $\delta \approx \alpha$, and this gives an opportunity to estimate τ_φ. No significant difference between the two crossover temperatures is considered [13]. In contrast to the HL theory, the 3D fluctuation region in well-structured YBCO films [16] has been found to be described by the 3D term of the AL theory [14],

$$\sigma'_{AL} = \{e^2/[32h\xi_c(0)]\}\varepsilon^{-1/2}. \qquad (7)$$

No LD fluctuation mechanism is observed in this case, as was mentioned above. It is clear on physical grounds that with increasing temperature the 3D fluctuation regime will persist until $\xi_c(T) \geq d$ [16]. Hence, in this case the 2D–3D crossover should occur at $\xi_c(T) \approx d$ or at

$$\xi_c(0) \approx d\varepsilon_0^{1/2}, \qquad (8)$$

which is twice as large as predicted by the LD and HL theories (Eq. (5)). Besides, the crossover at T_0 prooves to be of the MT–AL type [16].

Actually, Eq. (7) depends only on $\xi_c(0)$, which is independently determined by the measured value of ε_0 (Eq. (8)), thus noticeably reducing the number of fitting parameters. However, τ_φ (Eq. (6)) still remains uncertain, since neither l nor $\xi_{ab}(0)$ is directly measured in the FC experiment. To circumvent this problem we have designated $1.203(l/\xi_{ab}(0)) = \beta$ [16]. As before, to further evaluate $\tau_\varphi(100\text{ K})$ it is assumed that $\tau_\varphi(T) \sim 1/T$ and $\tau_\varphi T = \text{const}$ [7,15,16,27]. Hence, Eq. (6) can be rewritten as follows:

$$\tau_\varphi \beta T = \pi\hbar/(8k_B\varepsilon_0) = A\varepsilon_0^{-1}, \qquad (9)$$

where $A = \pi\hbar/(8k_B) = 2.988\cdot 10^{-12}$ s. Now the parameter $\tau_\varphi(100\text{K})\beta$ is strictly determined by the measured value of ε_0 and can be used in the fitting procedure together with $\xi_c(0)$. Besides $\delta_{\text{th}}(\varepsilon_0) = 2$ (Eq. (4)). Thus, the only fitting parameter now remains a *C*-factor introduced to take into account the structural imperfection of the sample [5]. But in contrast to Oh et al. [5], we introduce *C* as a factor by which Eqs. (2), (3) and (7) must be multiplied to fit the experimental data. It is clear that the farther *C* is from 1, the more influence of defects is expected [2]. However, independently of the measured values of the *C* factors, the ratio $C^* = C_{3D}/C_{2D} = (1.82 \pm 0.2)$ was found for all well-structured YBCO films with different oxygen concentration [2,16], as a result of the layered nature of HTSC.

Compared to OD YBCO films, the MT fluctuation mechanism in films with $T_c \le 82$ K (so-called 80-kelvin samples) is somewhat suppressed and partly substituted by the LD one because of the appearance of structural defects mostly produced by oxygen vacancies in the CuO chains, as described in detail in Ref. 2. The more defects, the more pronounced is the LD part of the $\sigma'(T)$ dependence and the greater is the suppression of the MT contribution. Nevertheless, the $\sigma'(T)$ dependence near T_c is still described by the 3D term of the AL theory (Eq. (7)). Naturally, $\sigma'(T)$ exhibits two dimensional crossovers in this case but just the second LD–AL (3D) crossover at ε_0 has been shown to determine $\xi_c(0)$ and $\tau_\varphi(100\ \text{K})\beta$ in 80-kelvin samples [2].

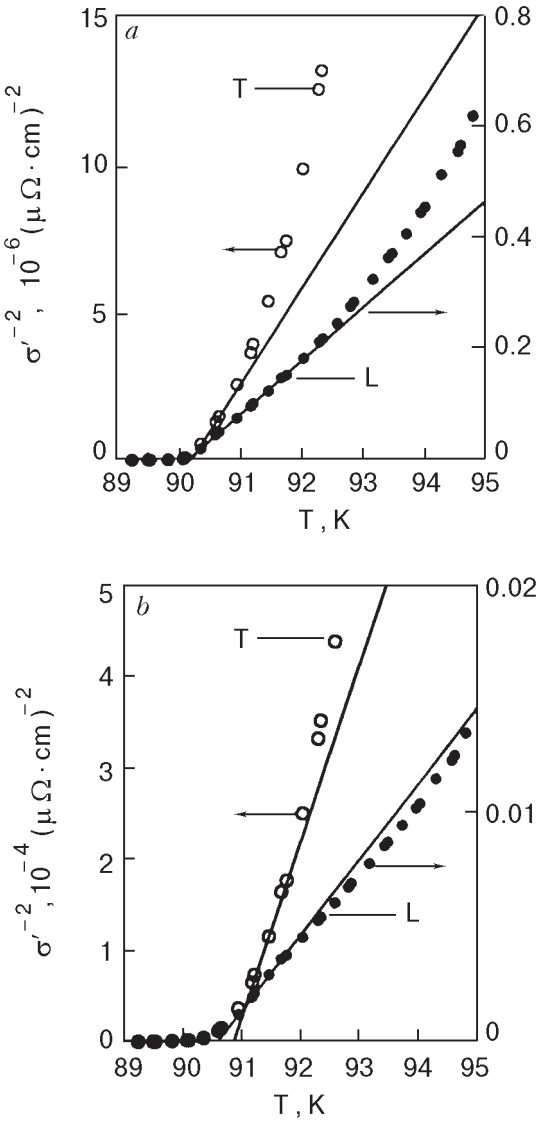

Fig. 2. σ'^{-2} vs T for samples M23 (*a*) and M35 (*b*) measured in the **L** (dots) and **T** (circles) direction, respectively; the solid lines is extrapolated 3D fluctuation regions.

3.1.2. Fluctuation conductivity analysis. Outside the critical region $\sigma'(T)$ is a function of $\varepsilon \approx (T - T_c^{mf})/T_c^{mf}$ only. Thus the determination of T_c^{mf} is of primary importance to the determination of $\sigma'(T)$. As before [2,16], T_c^{mf} is defined by extrapolating the linear 3D region of the σ'^{-2} vs T plot down to the **T** axis, since $\sigma'(T)$ should diverge as $(T - T_c^{mf})^{-1/2}$ (Eq. (7)) as T approaches T_c^{mf}. Figure 2 shows $\sigma'^{-2}(T)$ for samples M23 and M35 measured in the **L** and **T** directions. As expected, the each plot is characterized by a pronounced 3D region fitted by the straight line to determine T_c^{mf}. Above T_0 the data measured for M23-**L** (Fig. 2,*a*, dots) and the data measured for both samples in the **T** direction (Fig. 2,*a* and 2,*b*, circles) deviate to the left from the line. The fact means the absence of any MT fluctuation mechanism in this case [16]. On the other hand, the data measured for M35-**L** (Fig. 2,*b*, dots) demonstrate an evident rightward deviation from the line at T_0, thus suggesting the presence of the MT fluctuation mechanism in the sample in the latter case. But, strictly speaking, the deviation is relatively small in comparison with the well-structured OD films [16]. But the more striking result is the fact that the 3D region measured for M23-**T** turns out to be extremely short (Fig. 2,*a*, circles), resulting in $T_{0\mathbf{L}} - T_{0\mathbf{T}} \approx 0.9$ K (Fig. 2,*a*). Possible reasons for this finding will be discussed below.

Figure 3,*a* shows a plot of $\ln\sigma'$ vs $\ln\varepsilon$ (dots) for sample M23-**L** in comparison with the LD term of the HL theory (Eq. (2)) (curve *2*) and the 3D term of the AL theory (Eq. (7)) (curve *3*), as no MT fluctuation contribution is expected (Fig. 2,*a*). The LD–AL (3D) crossover, marked by the arrow on the figure, is distinctly seen on the plot at $\ln\varepsilon_0 \approx -3.98$ ($T_0 \approx 91.83$ K). Now the values $\xi_c(0) \approx (1.6 \pm 0.01)$ Å and $\tau_\varphi(100\ \text{K})\beta \approx 16.03 \cdot 10^{-13}$s can easily be determined using the measured ε_0 and Eqs. (8) and (9), respectively. The two parameters found enable us to reasonably fit the data in the whole temperature region of interest (Fig. 3,*a*). Besides, the value $\delta_{th}(\varepsilon_0) \approx 2$ is computed using Eq. (4), in good agreement with the above theoretical consideration. It has been established [16] that $\delta_{th}(\varepsilon_0) = 2$ only when ε_0, which determines both $\xi_c(0)$ and $\tau_\varphi(100\ \text{K})\beta$, is properly chosen. This criterion plays a significant role in the fitting procedure, especially when no MT contribution is observed.

Above T_0 the LD term with $C_{LD} = 0.82$ perfectly fits the data up to $\ln\varepsilon_{c0} \approx -2.98$ ($T_{c0} \approx$ $\approx$ 94.72 K) (Fig. 3,*a*, curve *2*). In accordance with the analysis for the 80-kelvin samples [2], observation of a fluctuation mechanism of the LD type can

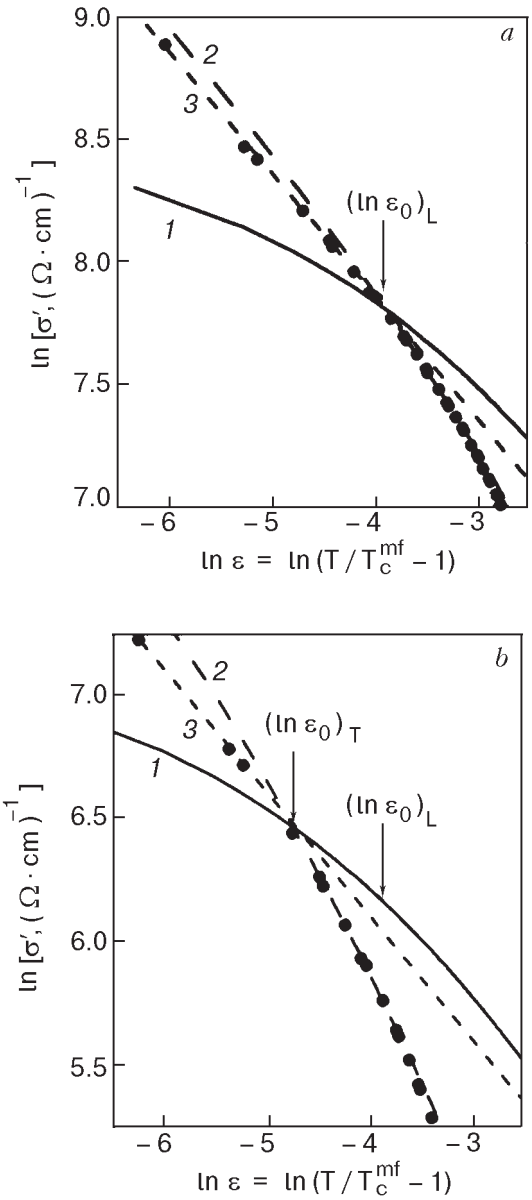

Fig. 3. a — $\ln\sigma'$ vs $\ln\varepsilon$ (dots) for sample M23-**L** ($T_c^{mf} = 90.14$ K) compared with fluctuation theories: curve *1* — MT term ($C_{2D} = 0.401$, $d = 11.7$ Å), *2* — LD term ($C_{LD} = 0.82$, $d = 11.7$ Å), *3* — AL(3D) term ($C_{3D} = 0.73$). *b* — $\ln\sigma'$ vs $\ln\varepsilon$ (dots) for sample M23-**T** ($T_c^{mf} = 90.19$ K) compared with fluctuation theories: curve *1* — MT term ($C_{2D} = 0.07$, $d = 17.34$ Å), *2* — LD term ($C_{LD} = 0.178$, $d = 35$ Å), *3* — AL(3D) term ($C_{3D} = 0.127$).

be considered as an evident sign of structural imperfection of a sample. Thus there should be a scatter of the intraplane distances in the sample even in the **L** direction as a result of the influence of defects throughout the relatively thick film. This conclusion is in good agreement with the results of the defect microstructure study discussed above. Simple algebra yields $d^* = \xi_c(0)/\varepsilon_{c0}^{1/2} \approx 7.2$ Å, and, as before, $d = 11.7$ Å at ε_0 is assumed [2]. Thus, the scatter appears to be just the same as had been found for 80-kelvin films [2]. Whether this is a coincidence or not has yet to be settled.

Below T_0 the LD model fails to fit the data because there is a rather pronounced linear 3D fluctuation region here, perfectly described by the 3D term of the AL theory with $C_{3D} = 0.73$ (Fig. 3,*a*, curve *3*). Thus, the observed crossover at T_0 is just of the LD–AL(3D) type expected to be responsible for the parameters of fluctuation analysis in the presence of defects [2]. For more assurance the MT term calculated using the found values for $\xi_c(0)$ and $\tau_\varphi(100\text{ K})\beta$ is also plotted (Fig. 3,*a*, curve *1*). As expected [2], when drawn with $C_{2D} = C_{3D}/1.82 \approx \approx 0.401$, it intersects the data just at the crossover point, accordingly marked as $\ln\varepsilon_0$ on the graph. This result once again comfirms the universality of the $C^* = 1.82 \pm 0.2$ ratio for the high-T_c oxides [2]. Nevertheless, the real MT fluctuation mechanism is completely suppressed here, being replaced by the LD one because of the presence of growth-related defects. The result of the structural imperfection is the observed diminution of the C_{3D} factor, expected to be close to 1 for well-structured OD YBCO systems [16]. We think that the $\sigma'(T)$ dependence found without any MT contribution but with clear LD–AL(3D) crossover appears to be typical for YBCO films with highly ordered defects. When defects are randomly distributed in the sample the crossover is never observed. In the latter case the data are traditionally fitted using the LD model alone [4–9], as was mentioned above.

Despite the fact that the set of defects in sample M35 was found to be the same [24], the FC behavior measured for sample M35-**L** appears to be rather different. Figure 4,*a* shows a $\ln\sigma'$ vs $\ln\varepsilon$ plot (dots) for sample M35-**L** compared with the theory in the established manner. Here the 3D region is somewhat shorter and the crossover at $\ln\varepsilon_0 \approx -4.39$ ($T_0 \approx 91.72$ K) becomes clear only when the corresponding theoretical curves are properly drawn. Using the measured ε_0, the values $\xi_c(0) = (1.3 \pm 0.01)$ Å, $\tau_\varphi(100\text{K})\beta \approx 24.24 \cdot 10^{-13}$ s, and $\delta_{th}(\varepsilon_0) \approx 2$ can easily be derived from the experiment. The parameters found enable one to reasonably fit the data in the whole temperature region of interest (Fig. 4,*a*). As before, the 3D fluctuation region near T_c is well described by the 3D AL term (Fig. 4,*a*, curve *3*) with $C_{3D} \approx 0.31$. However, above T_0 the fitting process turns out to be more complicated than before. As can be easily seen from the figure, the LD term (curve *2*), reduced to the crossover temperature, does not fit the

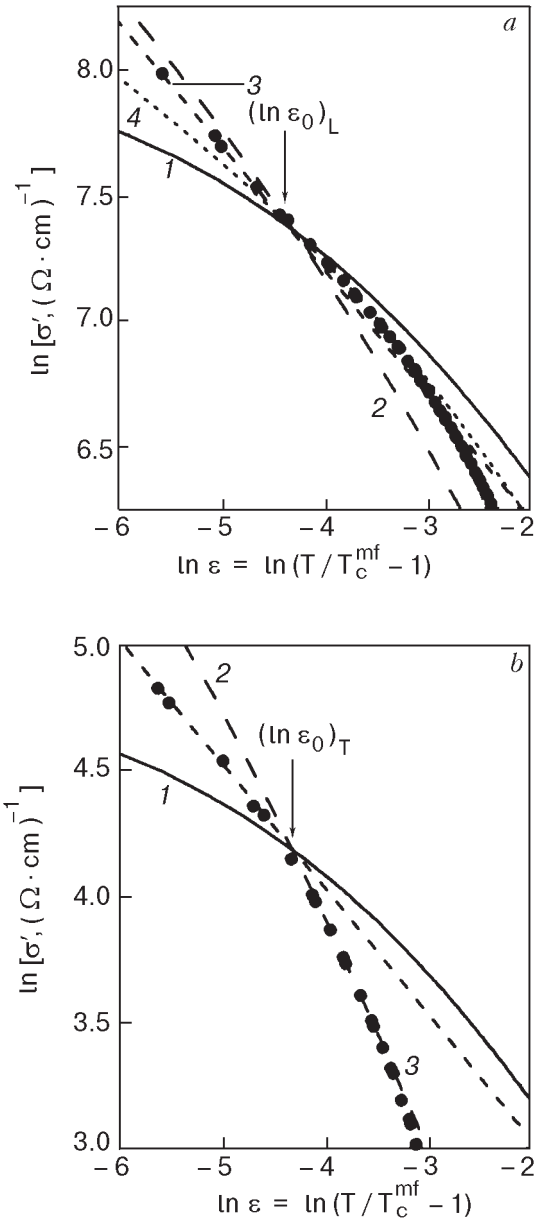

Fig. 4. *a* — $\ln\sigma'$ vs $\ln\varepsilon$ (dots) for sample M35-**L** ($T_c^{mf} = 90.60$ K) compared with fluctuation theories: curve *1* — MT term ($C_{2D} = 0.172$, $d = 11.7$ Å), *2* — LD term ($C_{LD} = 0.353$, $d = 11.7$ Å), *3* — AL(3D) term ($C_{3D} = 0.31$), *4* — MT+LD term ($C = 0.116$, $d = 11.7$ Å). *b* — $\ln\sigma'$ vs $\ln\varepsilon$ (dots) for sample M35-**T** ($T_c^{mf} = 90.85$ K) compared with fluctuation theories: curve *1* — MT term ($C_{2D} = 0.00714$, $d = 11.7$ Å), *2* — LD term ($C_{LD} = 0.0238$, $d = 35$ Å), *3* — AL(3D) term ($C_{3D} = 0.013$).

data in any temperature region. To complete the analysis the MT term, calculated using the values for found $\xi_c(0)$ and $\tau_\varphi(100\ \text{K})\beta$, is traditionally plotted (Fig. 4,*a*, curve *1*). As before, when drawn with $C_{2D} = C_{3D}/1.82 \approx 0.172$, it also intersects the data just at the crossover point. But in spite of the fact that the presence of the MT fluctuation contribution is evident from Fig. 2,*b*, the MT term also does not meet the case. Actually, all three theoretical mechanisms evidently fail to fit the data in the 2D fluctuation region. In the end, all the way up to $\ln\varepsilon_{c0} \approx -3.15$ ($T_{c0} \approx 94.48$ K), the data are found to be well fitted by the summary curve MT+LD (Fig. 4,*a*, curve *4*).

Fluctuation behavior of the MT+LD type but without crossover, likely overlooked by the authors, is reported for single crystals [7] and some YBCO films [9]. Thus a certain amount of the growth-related defects, likely produced by twins [7] or a slight degree of substrate miscut [9], has to be present in the samples. In our case the structural imperfection is apparently much stronger because of using the specific 10° miscut substrates, as is confirmed by the very small values of the C factors measured in the experiment. Besides, ΔT and $\rho(100\ \text{K})$ are about 2.2 times the value found for M23-**L**, whereas the ratio $\rho_{\mathbf{T}}(100\ \text{K})/\rho_{\mathbf{L}}(100\ \text{K})$ is 3 times larger, respectively (Table). All these facts evidently indicate the enhanced role of the defects in the sample. That is why even the partial observation of the MT fluctuation contribution here turns out to be somewhat controversial.

At first sight the observed $\sigma'(T)$ dependence of the MT+LD type is difficult to explain in terms of the FC approach discussed here. Indeed, as is well established now [2], the MT fluctuation mechanism gains importance in the distinct 2D fluctuation region and requires CuO_2 planes to be intact and regularly situated with an intraplane distance $d \approx 11.7\ \text{Å} > \xi_c(T)$, whereas the LD mechanism is found to be typical for samples with a noticeable spread of the intraplane distances and somewhat deteriorated planes. Thus, one have to assume that the growth-related defects result in some very specific sample structure, in which both the MT and LD fluctuation mechanisms are able to exist in parallel when measurements are performed in the **L** direction. As follows from a structural analysis [24], the sample surface looks like a remarkably regular, row-like terrace structure. The observed FC behavior makes it sure that between the rows the planes are presumably fully intact, giving rise to the MT fluctuation contribution. On the other hand, the planes are expected to be badly deteriorated on the tops of the rows. These parts of the sample are to be responsible for the appearance of the LD fluctuation mechanism. Despite the fact that the measurements are carried out in the **L** direction, the measuring current should evidently pass through both sample regions discussed, giving rise to the observed MT+LD combined fluctuation

behavior (Fig. 4,*a*, curve *4*). Thus, influence of the defects appears to be rather specific in this case. With increasing sample thickness (e.g., for the sample M23-**L**) the regions with mixed planes are likely to overlap. Naturally, no MT fluctuation mechanism will be observed in this case (Fig. 3,*a*). Whether or not the difference in the FC behavior found for the miscut-grown films is really due solely to the more than twofold difference in the samples thickness has yet to be settled.

Unfortunately, miscut-grown films for Hall effect measurements have not been prepared. As a result, the absolute value of $\beta \sim l/\xi_{ab}(0)$ remains unknown, giving us no possibility of directly deriving the explicit value of $\tau_\varphi(100\ \mathrm{K})$ from experiment. However, for sample M23-**L** there is an evident correlation between the ratio $T_c(\mathrm{M23\text{-}L})/T_c(\mathrm{F1}) = 1.03$ and $\xi_c(0)(\mathrm{F1})/\xi_c(0)(\mathrm{M23\text{-}L}) = 1.031$, respectively, suggesting that the value found for $\xi_c(0)$ is in good agreement with the conventional superconducting theory [28] as to the relationship between ξ and T_c:

$$\xi_0 \sim \hbar v_F/[\pi\Delta(0)], \qquad (10)$$

where v_F is the Fermi velocity and $\Delta(0)$ is the order parameter at $T = 0$ K (F1 is the well-structured YBCO film with $T_c = 87.8$ K (Ref. 16), considered to be the principal sample). Assuming $\xi_0 = \xi_c(0)$ and taking into account that $2\Delta(0) \approx 5k_BT_c$ for YBCO systems [29], one can rewrite Eq. (10) as $\xi_c(0) = G/T_c$, where $G = 2K\hbar v_F/(5\pi k_B)$ and $K \approx$ $\approx 0{,}12$ is the coefficient of proportionality. A plot of $\xi_c(0)$ as a function of T_c is shown in Fig. 5 (solid line) for the value $G = 1.46 \cdot 10^{-6}$ Å · K computed for F1 [2]. The dots are the experimentaly measured $\xi_c(0)$ values for samples M23, M35, and four YBCO films with different oxygen concentrations (samples F1–F6 from Ref. 2, 16). With increasing T_c the value $\xi_c(0)$ gradually decreases in accordance with the theory (Fig. 5, dots), thus clearly suggesting the conclusion that the coupling mechanism of high-T_c superconductivity to a certain degree follows the conventional superconducting theory. At the same time the parameter $\tau_\varphi(100\mathrm{K})\,\beta$, computed for the same samples, is found to be a linear function of T_c (Fig. 5, circles). All the data are normalized to the value $\tau_\varphi(100\ \mathrm{K})\beta \approx 5.9 \cdot 10^{-13}$ s for sample F6 (Ref. 16) in this case in order to make scales coinside. Since both $\xi_c(0)$ and $\tau_\varphi(100\mathrm{K})\,\beta$ are determined solely by ε_0, which is strictly determined by the crossover, the dependences found appear to be an inherent property of YBCO high-T_c oxides. As is clearly seen from the figure, sample M23-**L** perfectly matches both dependences shown at the highest temperature, in this way playing the role of the real OD system.

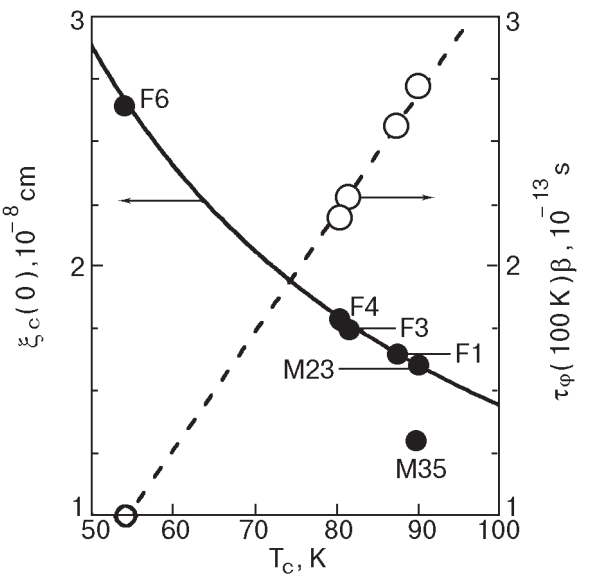

Fig. 5. $\xi_c(0)$ as a function of T_c (dots); the solid line represents the theory. Circles — $\tau_\varphi(100\,\mathrm{K})\beta$ vs T_c; the dashed line is a guide for the eye.

Summarizing the facts, it seems to be rather reasonable to ascribe to M23-**L** the same $\tau_\varphi(100\mathrm{K}) \approx$ $\approx 3.35 \cdot 10^{-13}$ s as was found for all other films [16]. The assumption could explain the fact that no significant diminution of the PG region is observed in this case (Fig. 1). Taking found τ_φ into account one can easily derive the value $\beta \approx 4.785$ from the measured $\tau_\varphi(100\mathrm{K})\beta$. Since $\xi_{ab}(0) = 13$ Å for F1 [16], the values $\xi_{ab}(0) = 13/1.03 = 12.62$ Å and $l = \xi_{ab}(0)\beta/1.203 = 51.7$ Å can easily be obtained for M23-**L**. Both calculated β and l are in good agreement with the FC analysis [16], for which evident increase of β and l with increasing T_c is observed. The result evidently confirms the assumption and suggests the conclusion that the fluctuating coupling mechanism in HTSC, leading to the appearance of fluctuation conductivity, has the same physics for all samples studied. But, on the other hand, the result looks somewhat surprising in view of the expected influence of the defects on the sample structure, and the estimated $l \approx 51.7$ Å looks suspiciously large for the same reason. To avoid this problem one have to assume that influence of the growth-related defects on the scattering of the normal charge carriers (which is responsible for the resistivity) and on the fluctuating pairing (which determines T_c) is not very considerable here, at least when measurements are performed in the **L** direction. This conclusion seems reasonable since sample M23-**L** has the lowest resistivity, the highest T_c, and relatively large values of the C factors as compared to the samples F1–F6 [2,16]. Besides,

the resistive transition is very narrow (Table) and, additionally, found $T_{*0} \approx 130$ K is very close to that predicted by the NAFL theory for OD YBCO systems [15]. The only exception is the absence of a clear MT fluctuation mechanism, which unexpectedly turns out to be the only evidence of the presence of defects in this case.

Strictly speaking, both $\xi_c(0)$ and $\tau_\varphi(100\,\mathrm{K})\beta$ found for M35 are not inconsistent with the dependences shown in Fig. 5. However, as it is easily seen from the figure, the absolute values of the parameters evidently do not match any of the plots shown. Especially $\tau_\varphi(100\,\mathrm{K})\beta \approx 24.24 \cdot 10^{-13}$ s proves to be extremely large. As a result, there are no reasonable assumptions as to how to get credible values of β and $\tau_\varphi(100\,\mathrm{K})$ in this case. Nevertheless, $\tau_\varphi(100\,\mathrm{K})$ is expected to be rather high. As a result, the PG temperature region determined by the measured $T_{*0\mathbf{L}} \approx 150$ K is the same as usually observed for OD YBCO films [3,9].

As expected, results of the FC measurements, obtained from the **T**-direction experiment, appear to be noticeably different. Figure 4,*b* shows a plot of $\ln\sigma'$ vs $\ln\varepsilon$ (dots) for the sample M35-**T** compared with the fluctuation theories. As it is easily seen, the absolute value of σ' is deeply suppressed, and, as expected, the C factors are extremely small, evidently reflecting the enhanced role of the defects in this case. It is easy to compute that $S^* = \sigma'_{\mathbf{L}}\,(92\ \mathrm{K})\,/\,\sigma'_{\mathbf{T}}(92\ \mathrm{K}) = 28.8$, whereas $\rho^* = \rho_{\mathbf{T}}(92\,\mathrm{K})/\rho_{\mathbf{L}}(92\,\mathrm{K}) = 10.48$ only. The corresponding values of S^* and ρ^*, found for sample M23, are 8.48 and 3.44, respectively. Here $T = 92$ K is chosen as a representative temperature which is close to the measured T_0 for each sample. Despite the fact that the absolute values of the parameters are noticeably different, the ratio S^*/ρ^* is approximately the same for both samples, namely 2.75 and 2.47, respectively. The finding apparently means that the relative diminution of the paraconductivity is approximately the same for both of the films discussed suggesting that the same mechanism of FC suppression occurs in each sample. It should be noted that $[\rho_N(T) - \rho(T)]$ (Eq. (2)), measured for both films in both directions, is of the same order. Hence, the observed diminution of σ' is actually the consequence of the corresponding increase of the **T** resistivity, as $\sigma' \sim 1/[\rho_N \rho(T)]$ (Eq. (2)). Besides, $\sigma'(T)$ drops to zero at $T_{*0} \approx 105$ K (Table), which is much lower than that measured in the **L** direction. Thus, the PG temperature range turns out to be rather limited in this case, as was mentioned above.

Nevertheless, despite the strong influence of defects, the standard linear $\sigma'(T)$ dependence, well described by the 3D AL term, but with $C_{3D} = 0.013$ only, is observed near T_c (Fig. 4,*b*, curve *3*). As before, the LD–AL (3D) crossover is distinctly seen on the plot at the same $\ln\varepsilon \approx -4.393$ as was measured for M35-**L**. Thus, the same values $\xi_c(0) \approx \approx (1.3 \pm 0.01)$ Å, $\tau_\varphi(100\,\mathrm{K})\beta \approx 24.24 \cdot 10^{-13}$ s, and $\delta_{\mathrm{th}} \approx 2$ are derived from the analysis, which seems reasonable. To check the type of crossover, the MT term calculated using the values found for $\xi_c(0)$ and $\tau_\varphi(100\,\mathrm{K})\beta$ is also plotted (Fig. 4,*b*, curve *1*). As before, when drawn with $C_{2D} = C_{3D}/1.82 \approx \approx 0.0072$, it intersects the data just at the crossover point, accordingly marked as $\ln\varepsilon_0$ on the graph. This finding indicates that the crossover is of just the type that has to determine the parameters of the fluctuation analysis [2], and it once again confirms the universality of the ratio $C^* \approx 1.82$ found for YBCO oxides [16]. Nevertheless, the MT curve runs far away from the experimental data, which is not surprising since the CuO_2 planes are expected to be badly mixed in the **T** direction. But, surprisingly, the LD term (not shown to prevent obscuring the graph) when drawn with $\xi_c(0) \approx \approx (1.3 \pm 0.01)$ Å and the value $d = 11.7$ Å commonly used in the FC analysis does not fit the data in any temperature region below or above T_0. After many trials it was eventually found that above T_0, all the way up to $\ln\varepsilon_{c0} \approx -3.3$ ($T_{c0} \approx 94.2$ K), the data can be perfectly extrapolated by the LD term with $\xi_c(0) \approx (1.3 \pm 0.01)$ Å but $d = (35 \pm 1)$ Å (Fig. 4,*b*, curve *2*). At first sight the result looks somewhat puzzling, but sample M23-**T** demonstrates exactly the same FC behavior above T_0 (Fig. 3,*b*, curve *2*). Moreover, the similar $\sigma'(T)$ dependence above T_0, fitted by the LD term with $d \approx 35$ Å, was recently found for YBCO films which structure was artificially deteriorated to increase the critical currents [30]. Thus, the specific temperature dependence found for the fluctuation conductivity above T_0 appears to be universal for the YBCO oxides with defected structure. As the CuO_2 planes are expected to be badly mixed in the **T** direction, it seems reasonable to consider this temperature region as a pseudo-two-dimensional one.

To account for this finding one have to assume that any new structure with the intraplane distance $d \approx 35$ Å is realized in the films as a result of the growth-related defects presence. However, this most simple explanation proves to be somewhat contradictory since the **L**-direction measurements indicate that $d = 11.7$ Å, and just this value of d is used in computing $\xi_c(0)$ and $\tau_\varphi(100\,\mathrm{K})\beta$ from the

T-direction experiment. Unfortunately, the 3D AL term (Eq. (7)) does not depend on d and cannot help solve the problem. Finally, before proceeding with assumptions it seems rather reasonable to find out the features of the FC behavior common to both of these films above T_0. Such a feature is the faster diminution of σ' with T in this temperature interval as compared with the **L**-direction experiment. As a result, $\sigma'(T)$ steepens, suggesting enhanced pair-breaking in the pseudo-two-dimentional region. In accordance with the discussion of the 80-kelvin films [2], this $\sigma'(T)$ dependence is to be described solely by the LD model, as a large spread of the intraplane distances in the **T** direction is expected. Strictly speaking, it is difficult to distinguish any predominant distance in this case. Taking all of the above remarks into account, the value $d = 35$ Å is obviously not to be considered as the distance between the conducting layers but has only to reflect the fact that the scattering rate of the fluctuating pairs, measured in the **T** direction above T_0, is at least 3 times that measured in the **L** direction (see Eq. (2)). As a result, the pseudogap temperature range measured in the **T** direction for both films turns out to be rather limited (Fig. 1), with $T_{*0\mathbf{L}} - T_{*0\mathbf{T}} \approx 20–45$ K (Table). This finding permits to conclude that the PG phenomenon, at least in OD YBCO oxides, is mainly governed by the fluctuating pairing.

At first sight sample M23-**T** exhibits just the same FC behavior (Fig. 3,*b*, dots). Above T_0, all the way up to $\ln\varepsilon_0 \approx -3.7$ ($T_{c0} \approx 92.41$ K), the $\sigma'(T)$ curve is well described by the LD model with $d = 35$ Å (Fig. 3,*b*, curve *2*), as mentioned above. But the LD–AL(3D) crossover unexpectedly occurs at $T_{0\mathbf{T}} < T_{0\mathbf{L}}$, resulting in the extremely short 3D region in this case. Really, only the leftmost few data points can be fitted by the 3D AL term with $C_{3D} = 0.127$ (Fig. 3,*b*, curve *3*) now. It looks as if all the data are shifted towards low temperatures compared with the **L**-direction experiment. The shift is distinctly seen on the graph as the difference between $\ln\varepsilon_{0\mathbf{T}}$ and $\ln\varepsilon_{0\mathbf{L}}$, also shown in the figure. The matter of whether we could again ascribe the shift to twice the difference in the samples thickness or whether it is an intrinsic feature of sample M23 has yet to be settled, leaving this an open question. Since the FC parameters are strictly determined by the ε_0, the shift evidently suggests the change of both $\xi_c(0)$ and $\tau_\varphi(100\,\mathrm{K})\beta$ compare with those measured for M23-**L**. Using the value found for $\ln\varepsilon_0 \approx -4.766$ ($T_0 \approx 90.95$ K), one can easily compute the values $\xi_c(0) \approx (1.08 \pm 0.01)$ Å and $\tau_\varphi(100\,\mathrm{K})\beta \approx 35.21 \cdot 10^{-13}$ s, suggesting the anisotropy of the parameters. But the anisotropy of $\xi_c(0)$ and the enlargement of τ_φ, appear to be rather unusual.

There are two possible approaches to estimation of $\xi_c(0)$ in the given case. The value $\xi_c(0) \approx (1.08 \pm 0.01)$ Å is computed from Eq. (7) taking $d = 11.7$ Å. The other possibility is the likely modification of d as a result of the influence of defects, considering $\xi_c(0)$ to be stable. Simple algebra (Eq. (8)) yields $d \approx 17.34$ Å in the latter case. Analysis of the defect microstructure [24] evidently shows that the crystal lattice is slightly tilted across the defects, and numerous stacking faults could result in a general change of the unit-cell height. That is why the second approach seems to be better, as it is difficult to see any physics behind the possible anisotropy of $\xi_c(0)$ depending on the measuring current direction in the *ab* plane. Finally, the AL and MT terms in the figure are drawn using $d = 17.34$ Å, and accordingly $\xi_c(0) = 1.6$ Å and $\tau_\varphi(100\,\mathrm{K})\beta \approx 35.21 \cdot 10^{-13}$ s. The only exception is $d = 35$ Å used for the LD fit. As expected, the AL and LD fits prove to be rather good in this case. And, as before, the MT term, drawn with $C_{2D} = C_{3D}/1.82 \approx 0.07$, intersects the data just at the crossover point (Fig. 4,*b*, curve *1*). Thus, it appears that, despite the strong influence of defects, the FC approach developed in Ref. 16 enables the reasonable description of the data in all of the temperature region of interest. As far as the noticeable enhancement of $\tau_\varphi(100\,\mathrm{K})\beta$ is concerned, we think the τ_φ should be the same as calculated for M23-**L**, since the same T_c is measured in both directions (Table), suggesting the fluctuating pairing in the 3D region to be independent of the presence of defects. The conclusion is confirmed by the fact that the temperature range of the 3D fluctuations observed for M35-**T** is the same as measured in the **L** direction (Fig. 4,*b*). Thus, the influence of defects is evidently much more stronger for the thicker sample. Therefore, to account for the enhancement of $\tau_\varphi(100\,\mathrm{K})\beta$ one can assume the enlargement of $\beta \sim l/\xi_{ab}(0)$. Naturally, some speculations as to the likely anisotropy of l, ξ_{ab}, and, finally, of the Fermi surface due to defect structure seem to be rather possible, but more experiments are evidently required to shed light on the problem.

4. Conclusion

As expected, the structural defects produced by 10° miscut growth of YBCO films [24] appear to deeply affect the fluctuation conductivity of the films, ultimately resulting in a rather complicated and somewhat contradictory picture of the FC be-

havior (Figs. 3 and 4). Nevertheless, the results are shown to be reasonably described within the framework of the FC analysis developed for the well-structured YBCO films [2,16].

Noticeable anisotropy of the FC behavior is found for both films studied, depending on whether measurements are performed in the **L** or in **T** direction. The FC measured in the **T** direction appears to be deeply suppresed. Moreover, above T_0 the scattering rate of the fluctuating pairs is estimated to be three times as large as measured in the **L** direction, suggesting enhanced pair-breaking in this case. As a result, the pseudogap temperature range measured in the **T** direction for both films (Fig. 1) turns out to be rather limited with $T_{*0\mathbf{L}} - T_{*0\mathbf{T}} \approx \approx 20 - 45$ K (Table). The finding permits to conclude that the PG phenomenon, at least in OD YBCO oxides, is mainly governed by the fluctuating pairing.

In the fluctuation region below T_0, where the 3D volume FC is realized, the pair-breaking mechanism appears to be the same for all samples studied, resulting in the same and very high T_c's. As a result, independently of the direction of measurements, the FC in the 3D fluctuation region near T_c is always fitted by the 3D term of the AL theory [14] and in all cases the ratio $C^* = C_{3D}/C_{2D} \approx (1.82 \pm 0.2)$ is held, as a result of the layered structure of HTSC. We think that both findings suggest the same fluctuating pairing mechanism near T_c for all YBCO oxides, independently of the presence of defect structure.

However, despite the fact that the same set of growth-related defects was found for both films studied [24], the FC behavior, especially that measured in the **L** direction, turns out to be rather different. Most likely the result can be attributed to the noticeable difference in the sample thickness d_0, as the difference in T_c is negligible (Table). Indeed, in the relatively thin film (sample M35) the influence of the defects on FC is not so pronounced. As a result, the fine structure of the $\sigma'(T)$ dependence, including all three AL, MT, and LD fluctuation contributions, is distinctly revealed on the plot (Fig. 4,*a*). In contrast with the FC results an enhanced scattering rate of the normal carriers, leading to a very high resistivity measured in the **T** direction, is observed in this case (Fig. 1). As a result, $d\rho/dT(\mathrm{M35}) \approx 2d\rho/dT(\mathrm{M23})$ is found, and, besides, the wider is ΔT, the larger is $\rho(T)$ and the ratio $\rho_{\mathbf{T}}/\rho_{\mathbf{L}}$ (Table).

With increasing film thickness (sample M23) the sample regions responsible for the different fluctuation contributions have to overlap (see the text), apparently leading to the averaging of the influence of defects on $\sigma'(T)$. As a result, the smooth $\sigma'(T)$ dependence described by the LD model alone is observed in this case (Fig. 3,*a*). At the same time, all resistivity parameters, including $d\rho/dT$ (Table), measured in the **L** direction turn out to be practically the same as those usually reported for the OD YBCO oxides [2,4–9]. Accordingly, $\rho_{\mathbf{T}}(100\,\mathrm{K})$ is about 6 times as less as measured for M35-**T**. We think all the findings have to corroborate this assumption.

Summarizing the facts, one may conclude that investigation of fluctuation conductivity additionally provides a useful method of getting reliable information on the inhomogeneity of the sample structure. Depending on what kind of $\sigma'(T)$ dependence is observed, additional information as to the type of defects and intensity of their influence on the resistivity and FC can easily be obtained. The method appears to be especially useful when no thorough structural analysis is unavailable.

Acknowledgements

The author acknowledges the staff of MPI-Stuttgart where experimental part of this work was done for their hospitality. He is also grateful to Prof. H.-U. Habermeier for stimulation of the study and fruitful suggestions, to T. Haage for films preparation and to Prof. V. M. Dmitriev for valuable comments in a discussion of the results of this study.

1. T. Timusk and B. Statt, *Rep. Prog. Phys.* **62**, 61 (1999).
2. A. L. Solovjov, H.-U. Habermeier, and T. Haage, *Fiz. Nizk. Temp.* **28**, 144 (2002) [*Low Temp. Phys.* **28**, 99 (2002)].
3. C. Carballeira, S. R. Curras, J. Vina, and J. A. Veira, *Phys. Rev.* **B63**, 144515-1 (2001).
4. P. P. Freitas, C. C. Tsuei, and T.S. Plaskett, *Phys. Rev.* **B36**, 833 (1987).
5. B. Oh, K. Char, A. D. Kent, M. Naito, M. R. Beasley, T. H. Geballe, R. H. Hammond, A. Kapitulnik, and J. M. Graybeal, *Phys. Rev.* **B37**, 7861 (1988).
6. T. A. Friedmann, J. P. Rice, John Giapintzakis, and D. M. Ginsberg, *Phys. Rev.* **B39**, 4258 (1989).
7. K. Winzer and G. Kumm, *Z. Phys. B. Condensed Matter* **82**, 317 (1991).
8. A. Gauzzi and D. Pavuna, *Phys. Rev.* **B51**, 15420 (1995)
9. W. Lang, G. Heine, P. Schwab, X. Z. Wang, and D. Bauerle, *Phys. Rev.* **B49**, 4209 (1995)
10. A. L. Solovjov, V. M. Dmitriev, H.-U. Habermeier, and I. E. Trofimov, *Phys. Rev.* **B55**, 8551 (1997) and references therein.

11. J. Axnas, B. Lundqvist, and O, Rapp, *Phys. Rev.* **B58**, 6628 (1998).
12. K. Maki, *Prog. Theor. Phys*. **39**, 897 (1968); R. S. Tompson, *Phys. Rev.* **B1**, 327 (1970).
13. S. Hikami and A. I. Larkin, *Mod. Phys. Lett*. **B2**, 693 (1998).
14. L. G. Aslamazov and A. I. Larkin, *Phys. Lett.* **A26**, 238 (1968).
15. B. P. Stojkovic and D. Pines, *Phys. Rev.* **B55**, 8576 (1997) and references therein.
16. A. L. Solovjov, H.-U. Habermeier and T. Haage, *Fiz. Nizk. Temp*. **28**, 24 (2002) [*Low Temp. Phys*. **28**, 17 (2002)].
17. W. E. Lawrence and S. Doniach, in: *Proc. of the Twelfth Int. Conf. on Low Temp. Phys.*, Kioto (1971), p. 361.
18. R. Knorpp, A. Forkl, H.-U. Habermeier, and H. Kronmuller, *Physica* **C230**, 128 (1994).
19. T. L. Hylton and M. R. Beasley, *Phys. Rev.* **B41**, 11669 (1990).
20. J. Mannhart, D. Anselmetti, J. G. Bednorz, A. Catana, Ch. Gerber, K. A. Muller, and D. G. Schlom, *Z. Phys*. **B86**, 177 (1992).
21. M. Oussena, P. A. J. de Groot, and S. J. Porter, *Phys. Rev.* **B51**, 1389 (1995).
22. H.-U. Habermeier, *Appl. Surf. Science* **69**, 204 (1993).
23. D. H. Lowndes, D. K. Christen, C. E. Klabunde, Z. L. Wang, D. M. Kroeger, J. D. Budai, Shen Zhu, and P. D. Norton, *Phys. Rev. Lett.* **74**, 2355 (1995).
24. T. Haage, J. Q. Li, B. Leibold, M. Cardona, J. Zegenhagen, and H.-U. Habermeier, *Solid State Commun*. **99**, 553 (1996).
25. J. B. Bieri, K. Maki, and R. S. Thompson, *Phys. Rev*. **B44**, 4709 (1991).
26. Y. B. Xie, *Phys. Rev*. **B46**, 13997 (1992).
27. Y. Matsuda, T. Hirai, and S. Komiyama, *Solid State Commun*. **68**, 103 (1988).
28. P.G. De Gennes, *Superconductivity of Metals and Alloys*, W. A. Benjamin, Inc., New York–Amsterdam (1966).
29. V. M. Dmitriev, A. L. Solovjov, and A. I. Dmitrenko, *Fiz. Nizk. Temp*. **15**, 356 (1989) [*Sov. J. Low Temp. Phys*. **15**, 200 (1989)].
30. V. M. Dmitriev, V. I. Stepanov, V. N. Svetlov, and A. L. Solovjov, to be published.